




Short Note

Diethyl [(4-((9*H*-carbazol-9-yl)methyl)-1*H*-1,2,3-triazol-1-yl)(benzamido)methyl]phosphonate

Serigne Abdou Khadir Fall ¹, Saïd Achamlale ^{1,2} , Younas Aouine ^{1,3} , Asmae Nakkabi ⁴, Hassane Faraj ¹ and Anouar Alami ^{1,*} 

¹ Engineering Laboratory of Organometallic, Molecular Materials and Environment (LIMOME), Faculty of Sciences Dhar El Mahraz, Sidi Mohammed Ben Abdellah University, Fez 30000, Morocco; serigneabdoukhadirfall@gmail.com (S.A.K.F.); achamlale@gmail.com (S.A.); anawr12000@yahoo.fr (Y.A.); hassanefaraj@yahoo.fr (H.F.)

² Laboratory of Scientific Research and Pedagogic Development (LSRPD) CRMEF Fez-Meknes, Meknes 50000, Morocco

³ Team of Organic Chemistry and Valorization of Natural Substances (COVSN), Faculty of Sciences, Ibn Zohr University, Agadir 80060, Morocco

⁴ Laboratory of Chemistry of Materials and Biotechnology of Natural Products, Faculty of Sciences, Moulay Ismail University, BP 11201, Meknes 50050, Morocco; asmaenakkabi@yahoo.fr

* Correspondence: anouar.alami@usmba.ac.ma; Tel.: +212-661-796-480; Fax: +212-535-733-171

Received: 5 November 2020; Accepted: 18 November 2020; Published: 20 November 2020



Abstract: The title compound, diethyl [(4-((9*H*-carbazol-9-yl)methyl)-1*H*-1,2,3-triazol-1-yl)(benzamido)methyl]phosphonate, was synthesized with excellent yield and high regioselectivity through 1,3-dipolar cycloaddition reaction between the α -azido diethyl amino methylphosphonate and the heterocyclic alkyne, 9-(prop-2-yn-1-yl)-9*H*-carbazole. The cyclization reaction by “click chemistry” was carried out in a water/ethanol solvent mixture (50/50), in the presence of copper sulfate pentahydrate and catalytic sodium ascorbate. The characterization of the structure of the resulting 1,4-regioisomer was performed by 1D and 2D-NMR experiments, infrared spectroscopy, and elemental analysis.

Keywords: triazole; α -amino phosphonic ester; click chemistry; carbazole; 2D-NMR spectroscopy

1. Introduction

For several decades, in the face of microbial resistance to antibiotics, there has been a strong rush to synthesize organophosphorus compounds [1], which are considered to be new bioisosters of amino carboxylic acids. The succession of N–C–P bonds gives α -amino phosphonic acids important electronic properties, such as the ability to have an acid–base behavior, in order to form a network of specific hydrogen bonds, which is very important in biological processes [2]. Thus, important biological and environmental properties of heterocyclic phosphonic amino acids have been identified in the literature [3]. They proved their relevance in the design of new formulae for osteoporosis drugs [4], as antimicrobial and antioxidant agents [5,6], anticancer compounds [7], and antibacterial compounds [8], but also in the study of corrosion inhibition [9,10]. Thus, methods for the synthesis of phosphonic amino acids bearing a heterocycle in the alpha position have been described [11,12]. However, their triazolic analogs remain very limited [13]. That is why we have been interested in their preparation. Continuing our investigations on the synthesis of heterocyclic phosphonic [14], we described in this paper our results concerning the synthesis of a new biheterocyclic phosphonic amino ester, namely diethyl [(4-((9*H*-carbazol-9-yl)methyl)-1*H*-1,2,3-triazol-1-yl)(benzamido)methyl]phosphonate. The approach adopted was to prepare, in a first step, the heterocyclic dipolarophile (2) by nucleophilic substitution of 9*H*-carbazole [15] on propargyl bromide. Next, we performed a 1,3-dipolar cycloaddition

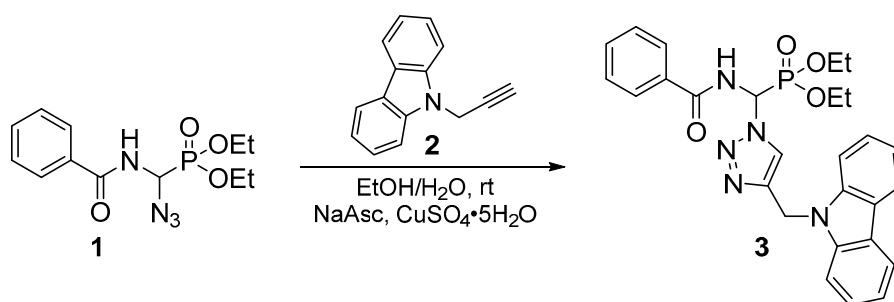
reaction by “click chemistry” [16,17] between diethyl (azido(benzamido)methyl)phosphonate (**1**) and 9-(prop-2-yn-1-yl)-9*H*-carbazole (**2**). The desired cycloadduct (**3**) was achieved regioselectively in high yield, and characterized by 1D-NMR (^{31}P , ^1H , ^{13}C), 2D-NMR (^1H - ^1H , ^1H - ^{13}C), IR, and elemental analysis (Supplementary Materials).

2. Results and Discussion

The azide dipole (**1**) was prepared according to a six-step synthesis, adopting the approach of Elachqar et al. [14]. This strategy requires anhydrous and inert operating conditions. The last step to obtain the azide dipole (**1**) was the action of sodium azide on the α -bromo- α -aminomethyl *N*-benzoylated diethyl phosphonate. The overall yield of this resynthesis strategy is 85%.

The product 9-(prop-2-yn-1-yl)-9*H*-carbazole (**2**) (CAS No. (4282-77-3)), used in the cycloaddition reaction, was resynthesized in 80% yield at our laboratory, according to the approach described in the literature [15], by nucleophilic substitution of propargyl bromide with carbazole.

The cyclization reaction by click chemistry was carried out by condensation of dipolarophile (**2**) and dipole azide (**1**) in a water/ethanol solvent mixture (50/50), in the presence of copper sulfate pentahydrate and catalytic sodium ascorbate (Scheme 1). The biheterocyclic derivative of the phosphonic analog of glycine was obtained with an excellent yield (90%), as a white solid after chromatography on a silica gel column (ethyl acetate/hexane: 1/1) and recrystallization in an ether/hexane mixture. The chemical structure of the title compound was confirmed by 1D and 2D-NMR, IR, and elemental analysis.



Scheme 1. Synthetic route for compound (**3**).

According to the Huisgen method [18] and previous work carried out in our research laboratory [19–22], the 1,3-dipolar cycloaddition reaction led to the formation of a regioisomeric mixture of 1,4- and 1,5-regioisomers, with a prevalence of the 1,4-regioisomer. However, under the conditions of click chemistry, depending on the nature of the metal ion used as a catalyst, the cycloaddition reactions selectively led to a single 1,4- or 1,5-regioisomer. Thus, in the presence of copper (II) ions [16], only the 1,4-regioisomer was obtained, whereas, in the presence of rhodium (I) [17], only the 1,5-regioisomer was obtained. For our part, during the cycloaddition reaction using copper (II) sulfate and sodium ascorbate, only the 1,4-regioisomer (**3**) was obtained, with an excellent yield (90%), as a white solid after chromatography on a silica gel column (ethyl acetate/hexane: 1/1), and recrystallization in an ether/hexane mixture. Its structure was established on the basis of decoupled and coupled ^{31}P -NMR (Figure 1), 1D ^1H and ^{13}C -NMR (Figures 2 and 3), homonuclear (^1H - ^1H) and heteronuclear (^1H - ^{13}C) 2D-NMR (Figures 4 and 5), infrared spectroscopy (Figure 6), and elemental analysis. Therefore, the cycloadduct (**3**) exhibits, in the decoupled ^{31}P -NMR spectrum (Figure 1A), a single signal at 13.26 ppm.

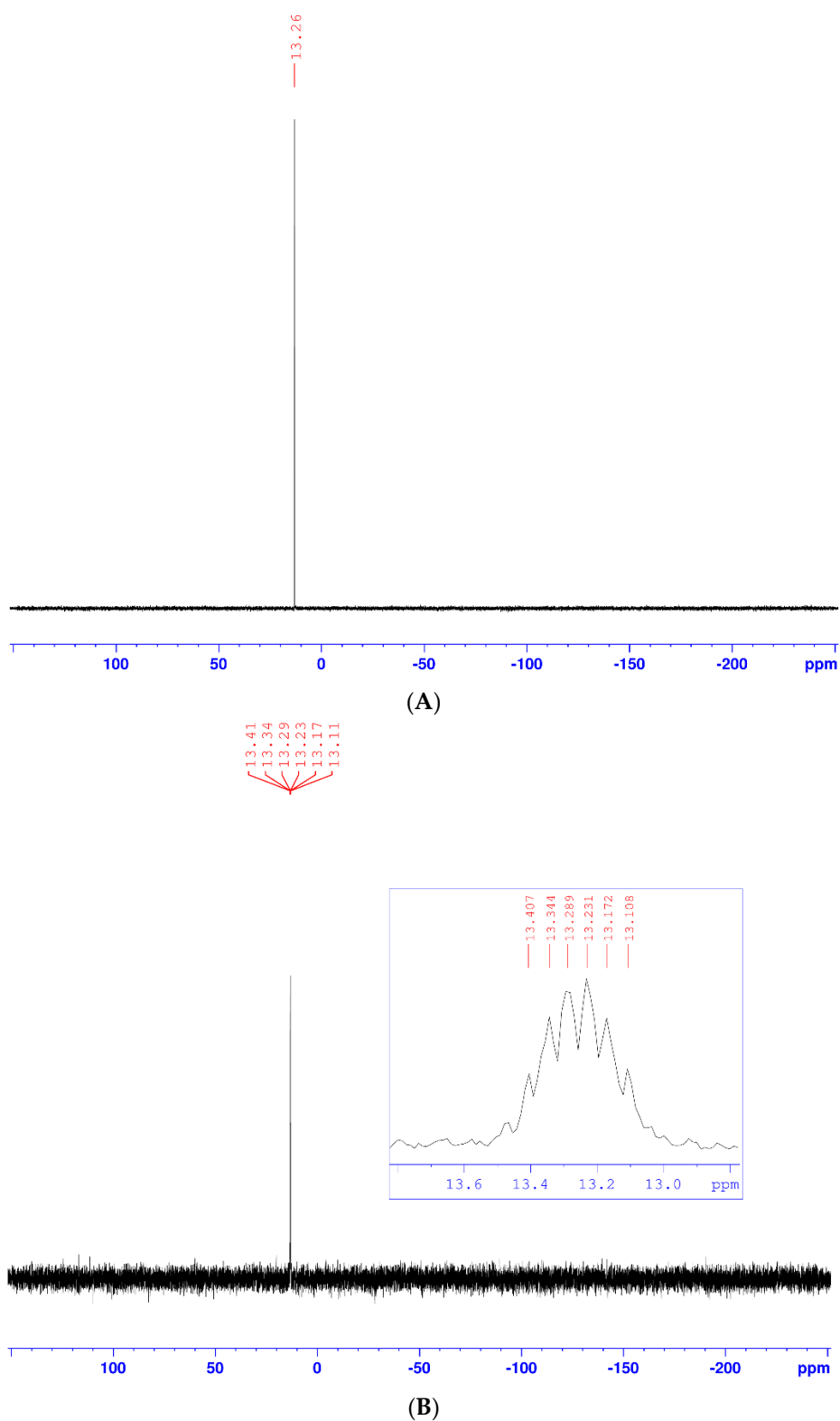


Figure 1. (A) Decoupled ^{31}P -NMR spectra of compound (3); (B) Coupled ^{31}P -NMR spectra of compound (3).

While it presents in the coupled ^{31}P -NMR spectrum (Figure 1B) a single signal centered at 13.27 ppm, the spread of this signal shows that it is a multiplet, because of the coupling of phosphorus with neighboring carbons and hydrogens.

In addition, in the ^{13}C -NMR spectrum (Figure 2), we note the coupling of phosphorus with the α carbon of the phosphonate ($^1J_{\text{C-P}} = 181.12\text{ Hz}$), and with the carbons of the two ethoxy groups which resonate as a doublet ($^2J_{\text{C-P}} = 11.3\text{ Hz}$ and $^3J_{\text{C-P}} \sim 6\text{ Hz}$).

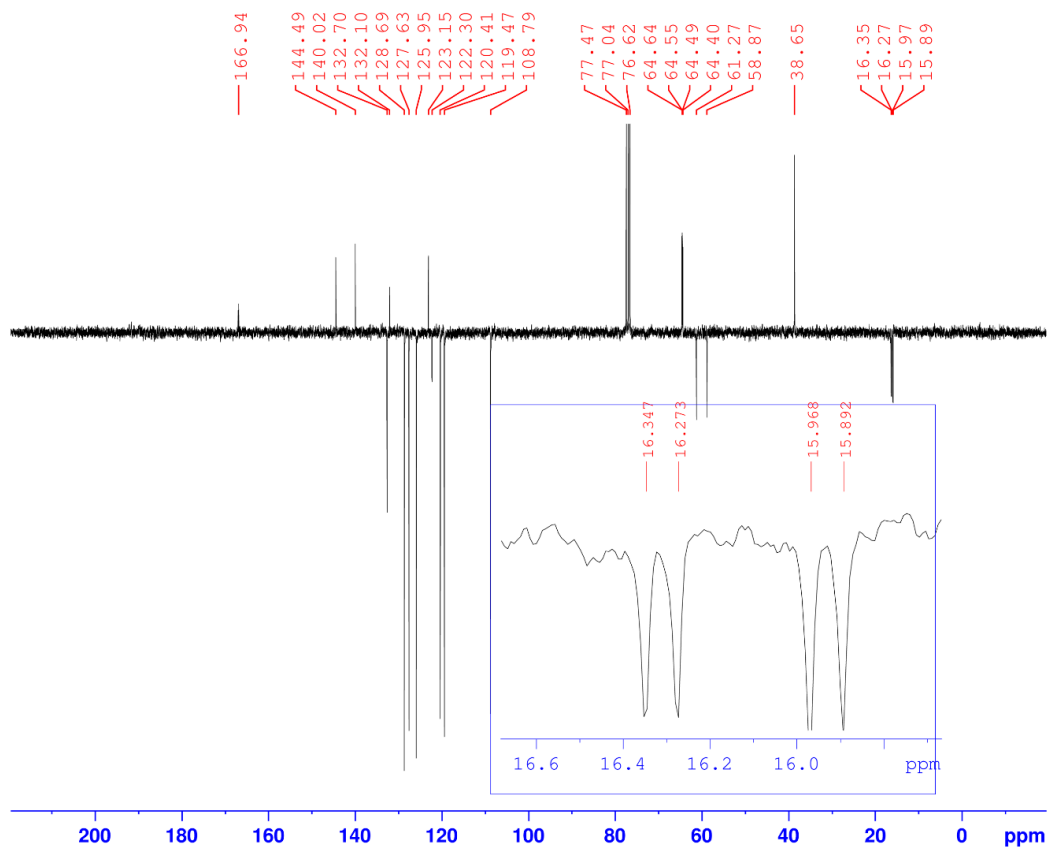


Figure 2. ^{13}C -NMR spectrum of compound (3).

While in ^1H -NMR (Figure 3), we note that the hydrogen carried by the α carbon of the phosphonate group appears as a doublet split, due to coupling with both amidic hydrogen $-\text{NH}$ and phosphorus ^{31}P , $^3J_{\text{H-H}} = 10\text{ Hz}$ and $^2J_{\text{H-P}} = 15.4\text{ Hz}$. While the two protons of the first ethoxy group OCH_2CH_3 resonate as a split quintuplet, due to coupling with both the three protons of the methyl group $-\text{CH}_3$ and phosphorus ^{31}P , $^3J_{\text{H-H}} = 7\text{ Hz}$ and $^3J_{\text{H-P}} = 1.5\text{ Hz}$. Finally, the two OCH_aH_b protons of the other ethoxy group resonate as two split sextuplets because the two protons H_a and H_b are not magnetically equivalent. The coupling constants are identical to the previous ones.

Moreover, the analysis of the homonuclear ^1H - ^1H 2D spectrum of compound (3) shows a perfect correlation between neighboring protons (Figure 4 and Table 1). It is important to specify that the two hydrogen atoms carried by the carbon atom $-\text{CH}_2-$ of the ethoxy group resonate as two split quintuplets, because the two protons H_a and H_b are not magnetically equivalent. This observation was confirmed in both mono- and heteronuclear 2D-NMR (Figures 4 and 5). The definite assignment the chemical shifts of protons and carbons are shown in Table 1.

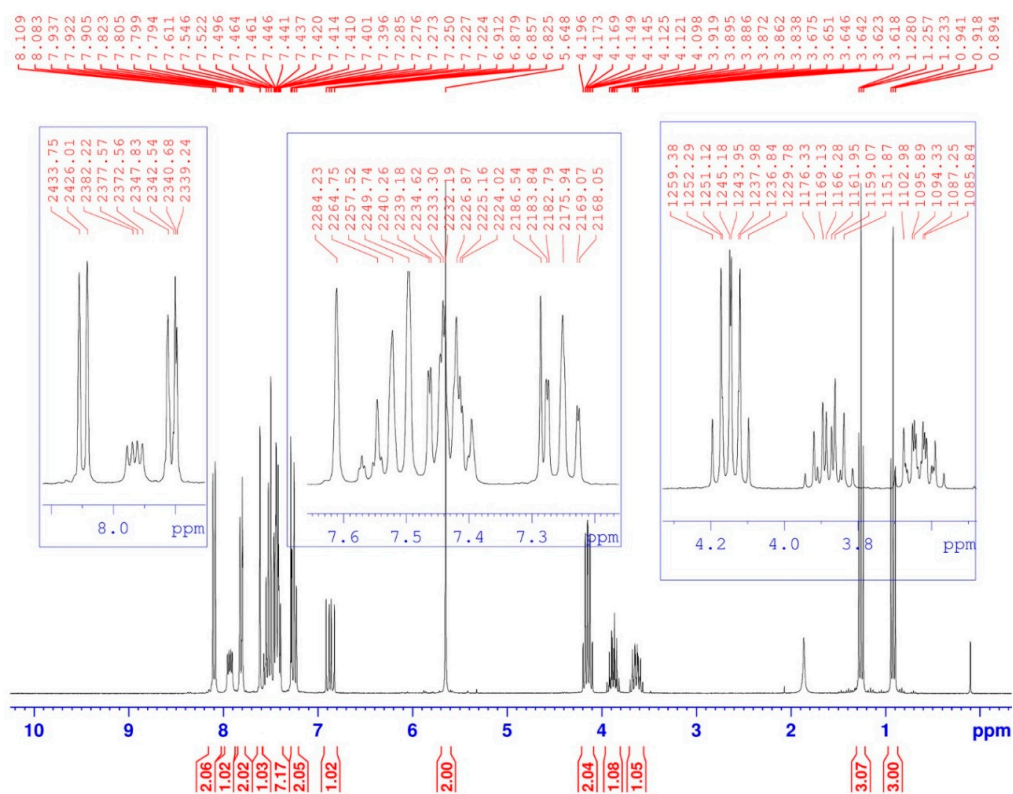


Figure 3. $^1\text{H-NMR}$ spectrum of compound (3).

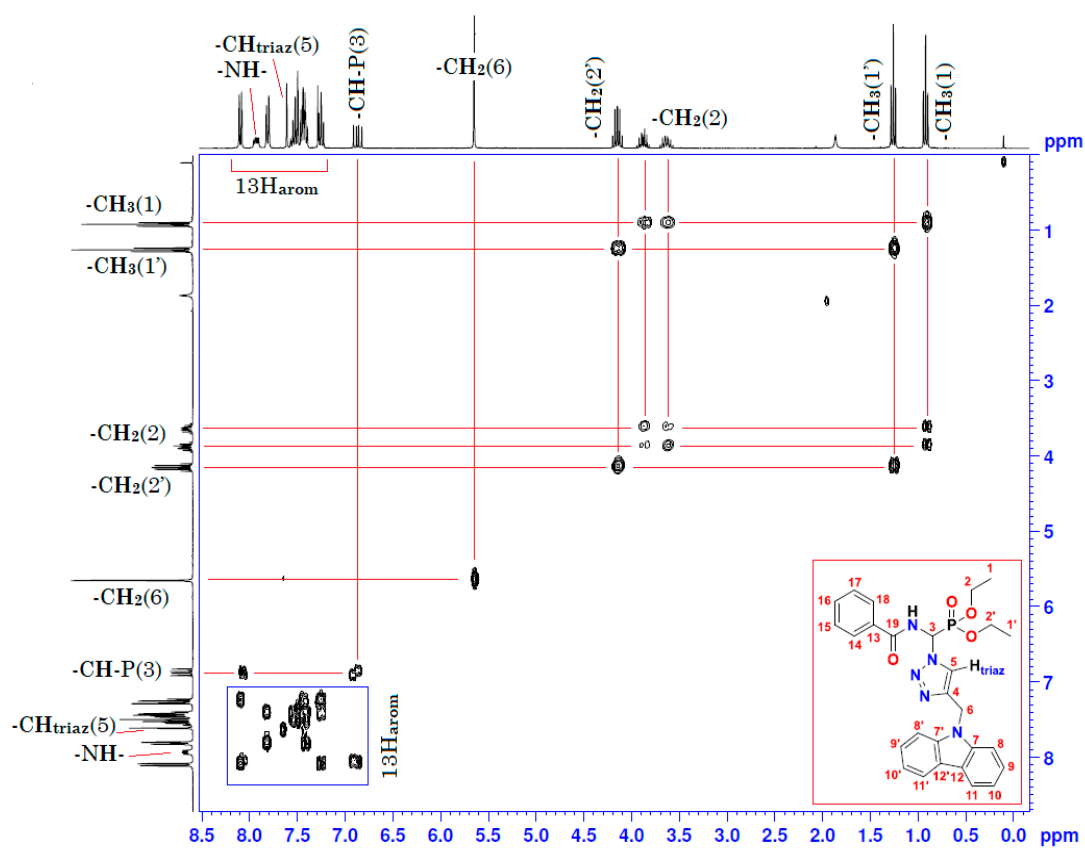


Figure 4. Homonuclear $^1\text{H-}^1\text{H}$ 2D spectrum of compound (3).

Table 1. ^1H (300 MHz) and ^{13}C (75 MHz) NMR spectral data for compound (3) in CDCl_3 , including results obtained by homonuclear 2D shift-correlated and heteronuclear 2D shift-correlated HMBC. Chemical shifts (δ in ppm) and coupling constants (J in Hz).

Position	δ_{H}	δ_{C}	Correlation H–H	Correlation C–H
1	0.92 (t, $^3J = 7$)	15.89–15.97 (d, $^3J_{\text{C-P}} = 5.7$)	$3\text{H}^1\text{-}3\text{H}^1$; $3\text{H}^1\text{-}2\text{H}^2$	$\text{C}^1\text{-}3\text{H}^1$
1'	1.26 (t, $^3J = 7$)	16.27–16.35 (d, $^3J_{\text{C-P}} = 6.8$)	$3\text{H}^{1'}\text{-}3\text{H}^{1'}$; $3\text{H}^{1'}\text{-}2\text{H}^{2'}$	$\text{C}^{1'}\text{-}3\text{H}^{1'}$
2	3.62–3.67 (m) 3.84–3.92 (m)	64.49–64.64 (d, $^2J_{\text{C-P}} = 11.3$)	$2\text{H}^2\text{-}2\text{H}^2$; $2\text{H}^2\text{-}3\text{H}^1$	$\text{C}^2\text{-}2\text{H}^2$
2'	4.10–4.20 (m)	64.40–64.55 (d, $^2J_{\text{C-P}} = 11.3$)	$2\text{H}^{2'}\text{-}2\text{H}^{2'}$; $2\text{H}^{2'}\text{-}3\text{H}^{1'}$	$\text{C}^{2'}\text{-}2\text{H}^{2'}$
3	6.82–6.91 (dd, $^3J_{\text{H-H}} = 10$; $^2J_{\text{H-P}} = 15.4$)	58.87–61.27 (d, $^1J_{\text{C-P}} = 181.1$)	$1\text{H}^3\text{-}1\text{H}^3$ $1\text{H}^3\text{-}1\text{H}_{\text{amide}}$	$\text{C}^3\text{-}1\text{H}^3$
4	-	144.49	-	-
5	7.61 (s)	122.30	$1\text{H}^5\text{-}1\text{H}^5$	$\text{C}^5\text{-}1\text{H}^5$
6	5.65 (s)	38.65	$2\text{H}^6\text{-}2\text{H}^6$	$\text{C}^6\text{-}2\text{H}^6$
7 and 7'	-	140.42	-	-
8 and 8'	8.08–8.11 (d, $J = 8$)	120.41	$1\text{H}^8\text{-}1\text{H}^8$ $1\text{H}^{8'}\text{-}1\text{H}^{8'}$	$\text{C}^8\text{-}1\text{H}^8$ $\text{C}^{8'}\text{-}1\text{H}^{8'}$
9 and 9' 13–18	7.40–7.55 (m)	108.79 120.41–132.70	$1\text{H}^9\text{-}1\text{H}^9$; $1\text{H}^{9'}\text{-}1\text{H}^{9'}$ 5H arom(Ph)-5H _{arom(Ph)}	$\text{C}^9\text{-}1\text{H}^9$; $\text{C}^{9'}\text{-}1\text{H}^{9'}$ 5C arom(Ph)-5H _{arom(Ph)}
10 and 10'	7.22–7.28 (m)	119.47	$1\text{H}^{10}\text{-}1\text{H}^{10}$ $1\text{H}^{10'}\text{-}1\text{H}^{10'}$	$\text{C}^{10}\text{-}1\text{H}^{10}$ $\text{C}^{10'}\text{-}1\text{H}^{10'}$
11 and 11'	7.79–7.82 (d, $J = 8$)	127.63	$1\text{H}^{11}\text{-}1\text{H}^{11}$ $1\text{H}^{11'}\text{-}1\text{H}^{11'}$	$\text{C}^{11}\text{-}1\text{H}^{11}$ $\text{C}^{11'}\text{-}1\text{H}^{11'}$
-NH-	7.90–7.95 (dd, $^3J_{\text{H-H}} = 9.66$; $^3J_{\text{H-P}} = 5.01$)	-	$1\text{H}_{\text{amide}}\text{-}1\text{H}_{\text{amide}}$ $1\text{H}_{\text{amide}}\text{-}1\text{H}^3$	-
19	-	166.94	-	-

The interpretation of the heteronuclear 2D-NMR spectrum of the cycloadduct shows a perfect correlation, between protons and adjacent carbons on the one hand, and between protons and neighboring carbons on the other hand (Figure 5 and Table 1). In addition, the 2D heteronuclear spectrum allowed us to confirm the proposed structure of the cycloadduct. Thus, these results are in perfect agreement with the literature data on “click chemistry” which attributes the structure of the product to the 1,4-regioisomer. This structure is also assigned on the basis of literature data on chemical shifts of triazolic protons [23,24]. The chemical shift of the triazolic proton in position 5 ($\delta_{\text{H}5}$) of the triazolic cycle is more deshielded than its counterpart in position 4 for the 1,5-regioisomer ($\delta_{\text{H}5} > \delta_{\text{H}4}$). Its signal is generally between 8 and 8.5 ppm. Thus, according to the ^1H - ^{13}C 2D heteronuclear spectrum of compound (3), the triazole proton at 7.61 ppm correlates perfectly with its adjacent carbon, which resonates in the ^{13}C -NMR at 122.30 ppm (Figure 5 and Table 1). The value of the chemical shift of the triazole proton in position 5 of our compound (3) is 7.61 ppm. This value is lower than the values described in the literature. This slight shielding can be explained by the effect of magnetic anisotropy due to the resonance caused by the delocalization of π -electrons from the carbazole ring. This resonance creates an induced magnetic field \mathbf{B} (\mathbf{B}_{ind}) which opposes the external magnetic field \mathbf{B}_0 of the NMR apparatus, giving rise to a lower effective magnetic field \mathbf{B} (\mathbf{B}_{eff}), and resulting in the shielding of all protons in the space of the two cones opposed by the summit, which lies in the middle of the horizontal plane of the carbazole ring. Consequently, the triazolic proton in position 5 may be found in this shielding area, which explains the value below 8 ppm ($\delta_{\text{H}5} = 7.61 < 8$ ppm). Conversely,

the protons of the two benzene rings of carbazole at 8, 8', 11, and 11' are in a horizontal plane, with an effective B_{eff} magnetic field resulting from the sum of B_0 and B_{ind} . The latter is the origin of the deshielding observed for its protons.

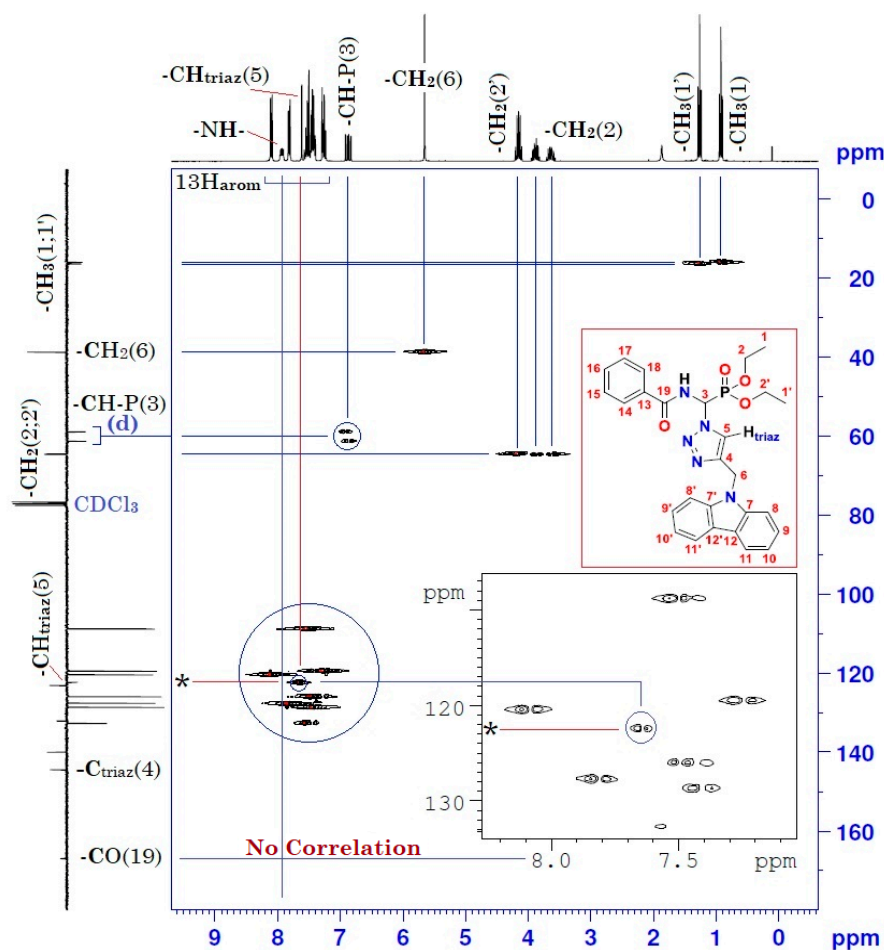


Figure 5. Heteronuclear ^1H - ^{13}C 2D spectrum of compound (3).

In addition, we obtained the infrared spectrum of the compound (3) (Figure 6). The assignments of the bands observed and the wavenumbers relative intensities are listed in Table 2.

Table 2. Bands assignments (cm^{-1}) in the IR spectrum of compound (3).

Liaison	Vibration	Wavenumber (cm^{-1})
C–H	$\nu_{(\text{Csp}^3\text{-H})}$	2850–3000
	$\delta_{(\text{Csp}^3\text{-H})}$	~1400
C=C	$\nu_{(\text{Csp}^2\text{-Csp}^2)}$	1500–1600
C–H _{aromatic}	$\nu_{(\text{Csp}^2\text{-H})}$	3000–3100
	$\delta_{(\text{Csp}^2\text{-H})}$	~985 and ~910
N–H _{amide}	$\nu_{(\text{N-H})}$	3050–3500
C=O _{amide}	$\nu_{(\text{C=O})}$	1650
C–N	$\nu_{(\text{C-N})}$	1020–1220
P=O	$\nu_{(\text{P=O})}$	1250
P–O–C	$\nu_{(\text{P-O-C})}$	1050

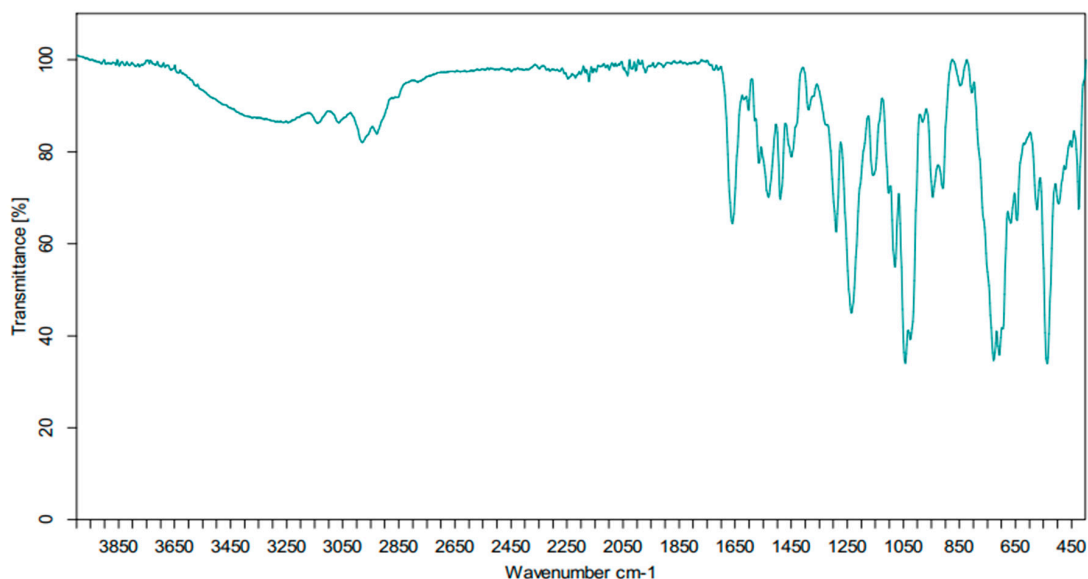


Figure 6. IR spectrum of compound (3).

The infrared spectrum of the cycloadduct (3) shows:

- Two bands in the range of 3050–3100 cm^{-1} , corresponding to the elongation vibrations of $\nu(\text{C}_{\text{sp}2}\text{-H})$.
- Two bands in the range of 2900–2950 cm^{-1} , corresponding to the elongation vibrations of $\nu(\text{C}_{\text{sp}3}\text{-H})$.
- One intense band around 1650 cm^{-1} , attributable to the C=O function.
- A strong band at 1250 cm^{-1} , corresponding to the valence vibrations of the $\nu(\text{P=O})$ function.
- A medium band at 1050 cm^{-1} , associated with the valence vibrations of the $\nu(\text{P-O-C})$ link.
- The observation of the bands around 850 and 900 corresponds to the deformation vibrations of $\nu(\text{N-H})$.

All these interpretations allowed us to propose for the cycloadduct (3), the nomenclature of the 1,4-regioisomer, which is diethyl [(4-((9*H*-carbazol-9-yl)methyl)-1*H*-1,2,3-triazol-1-yl) (benzamido)methyl]phosphonate.

3. Materials and Methods

All solvents were purified following the standard techniques and commercial reagents were purchased from Sigma-Aldrich (St. Louis, MO, USA). Melting point was determined with an electrothermal melting point apparatus and was uncorrected. NMR spectra (^1H and ^{13}C) were recorded on a Bruker AM 300 spectrometer (operating at 300.13 MHz for ^1H , at 75.47 MHz for ^{13}C) (Bruker Analytische Messtechnik GmbH, Rheinstetten, Germany). NMR data are listed in ppm and are reported relative to tetramethylsilane (^1H , ^{13}C); residual solvent peaks being used as an internal standard. All reactions were followed by thin-layer chromatography (TLC). TLC analyses were carried out on 0.25 mm thick precoated silica gel plates (Merck Fertigplatten Kieselgel 60F₂₅₄) and spots were visualized under UV light or by exposure to vaporized iodine. The FT-IR spectrum was recorded in KBr pellet on a Bruker Vertex 70 FTIR spectrometer. Elemental analysis was performed with a Flash 2000 EA 1112, Thermo Fisher Scientific-Elemental Analyzer (CNRST, Rabat, Morocco).

To a solution of 2.2 mmol of azide (1) and 2.2 mmol of alkyne (2) in 10 mL of an ethanol–water mixture (1/1), 0.05 equivalent of copper sulfate pentahydrate ($\text{CuSO}_4 \cdot 5\text{H}_2\text{O}$) was used as catalyst with 0.1 equivalent of sodium ascorbate (NaAsc). The reaction mixture was stirred for 24 h at room temperature. As soon as the reaction was completed, the precipitate formed was filtered, and the solvent was evaporated under reduced pressure. The resulting crude was washed with water and extracted with methylene chloride. The organic layer was dried over sodium sulfate (Na_2SO_4), and the solvent was removed under reduced pressure. The resulting oil was purified by column chromatography of silica gel (ethyl acetate/hexane).

Diethyl [(4-((9*H*-carbazol-9-yl)methyl)-1*H*-1,2,3-triazol-1-yl)(benzamido)methyl]phosphonate (3). Yield = 90% (White solid); R_f = 0.4 (ether/ methanol 5%); m.p. = 226–228 °C. $^1\text{H-NMR}$ (CDCl_3 , δ_{H} ppm): 0.92 (t, 3H, $-\text{CH}_2-\text{CH}_3$, $^3J = 7$ Hz), 1.26 (t, 3H, $-\text{CH}_2-\text{CH}_3$, $^3J = 7$ Hz), 3.62–3.67 (m, 1H, $-\text{OCH}_a\text{H}_b-\text{CH}_3$), 3.84–3.92 (m, 1H, $-\text{OCH}_a\text{H}_b-\text{CH}_3$), 4.1–4.2 (m, 2H, (P-O- CH_2-CH_3)), 5.65 (s, 2H, triaz- CH_2 -carbaz), 6.83–6.91 (dd, 1H, NH-CH-P, $^3J_{\text{H-H}} = 10$ Hz, $^2J_{\text{H-P}} = 15.4$ Hz), 7.22–7.27 (m, 2H_{arom}(carbaz)), 7.40–7.55 (m, 7H, 5H_{arom}(Ph) + 2H_{arom}(carbaz)), 7.61 (s, 1H, $-\text{CH}_{\text{triaz}}$), 7.79–7.82 (d, 2H_{arom}(carbaz), $J = 8$ Hz), 7.90–7.95 (dd, 1H, NH-CH-P, $^3J_{\text{H-H}} = 9.66$ Hz, $^3J_{\text{H-P}} = 5.01$ Hz), 8.08–8.11 (d, 2H_{arom}(carbaz), $J = 8$ Hz).

$^{13}\text{C-NMR}$ (CDCl_3 , δ_{C} ppm): 15.89–15.97 (d, 1C, $-\text{PO}-\text{CH}_2-\text{CH}_3$, $^3J_{\text{C-P}} = 5.7$ Hz), 16.27–16.35 (d, 1C, $-\text{PO}-\text{CH}_2-\text{CH}_3$, $^3J_{\text{C-P}} = 6.80$ Hz), 38.65 (1C, triaz- CH_2 -carbaz), 58.87–61.27 (d, 1C, $-\text{CH}-\text{P}$, $^1J_{\text{C-P}} = 181.12$ Hz), 64.40–64.55 (d, 1C, $-\text{PO}-\text{CH}_2-\text{CH}_3$, $^2J_{\text{C-P}} = 11.3$ Hz), 64.49–64.64 (d, 1C, $-\text{PO}-\text{CH}_2-\text{CH}_3$, $^2J_{\text{C-P}} = 11.3$ Hz), 108.79, 119.47, 120.41, 123.15, 125.95, 127.63, 128.69, 132.10, 132.70, 140.42 (18C, 6C_{arom}(Ph) + 12C_{arom}(carbaz)), 122.30 (1C, C_t(triaz)), 144.49 (1C, C_q(triaz)), 166.94 (1C, CO). IR ($\nu(\text{cm}^{-1})$): 3050 (N-H), 2850 (C_{sp3}-H), 1630 (C=O), 1250 (P=O), 1050 (P-OEt). Anal. Calcd. for C₂₇H₂₈N₅O₄P (%): C, 62.66; H, 5.45; N, 13.53; Found (%): C, 62.63; H, 5.47; N, 13.56.

4. Conclusions

In summary, the 1,3-dipolar cycloaddition reaction between azide (1) and the terminal heterocyclic alkyne (2) allows regioselective access to the 1,4-isomer, with excellent yield. The characterization of the structure of the diethyl [(4-((9*H*-carbazol-9-yl)methyl)-1*H*-1,2,3-triazol-1-yl)(benzamido)methyl]phosphonate was performed by different spectroscopic methods and elemental analysis. The heteronuclear 2D NMR allowed us to attribute the structure unequivocally by the observed correlations. This also converges with the data in the literature. The evaluation of the anti-corrosion and biological activities of the synthesized product is under way.

Supplementary Materials: Supplementary Materials of diethyl (azido(benzamido)methyl)phosphonate (1): Figure S1: $^1\text{H-NMR}$ spectrum of compound (1), Figure S2: $^{13}\text{C-NMR}$ spectrum of compound (1), Figure S3: Homonuclear $^1\text{H}-^1\text{H}$ spectrum of compound (1), Figure S4: Heteronuclear $^1\text{H}-^{13}\text{C}$ spectrum of compound (1); Supplementary Materials of 9-(prop-2-yn-1-yl)-9*H*-carbazole (2): Figure S1: $^1\text{H-NMR}$ spectrum of compound (2), Figure S2: $^{13}\text{C-NMR}$ spectrum of compound (2); Supplementary Materials of diethyl [(4-((9*H*-carbazol-9-yl)methyl)-1*H*-1,2,3-triazol-1-yl)(benzamido)methyl]phosphonate (3): Figure S1: Decoupled ^{31}P NMR spectrum of (3), Figure S2: Coupled ^{31}P NMR spectrum of (3), Figure S3: $^{13}\text{C-NMR}$ spectrum of compound (3), Figure S4: $^1\text{H-NMR}$ spectrum of compound (3), Figure S5: Homonuclear $^1\text{H}-^1\text{H}$ spectrum of compound (3), Figure S6: Heteronuclear $^1\text{H}-^{13}\text{C}$ spectrum of compound (3), Figure S7: IR spectrum of compound (3).

Author Contributions: S.A.K.F. performed the experiments; S.A., H.F. and A.A. conceived and designed the experiments; S.A., Y.A., A.N. and A.A. analyzed the data; S.A., Y.A. and A.A. wrote the paper. All authors have read and agreed to the published version of the manuscript.

Funding: This research received no external funding.

Acknowledgments: This work was supported by Sidi Mohammed Ben Abdellah University (USMBA) and National Center for Scientific and Technical Research (CNRST).

Conflicts of Interest: The authors declare no conflict of interest.

References

1. Elsherbiny, D.A.; Abdelgawad, A.M.; El-Naggar, M.E.; El-Sherbiny, R.A.; El-Rafie, M.H.; El-Sayed, I.E.-T. Synthesis, antimicrobial activity, and sustainable release of novel α -aminophosphonate derivatives loaded Carrageenan Cryogel. *Int. J. Biol. Macromol.* **2020**, *163*, 96–107. [[CrossRef](#)] [[PubMed](#)]
2. Mucha, A.; Kafarski, P.; Berlicki, Ł. Remarkable potential of the α -aminophosphonate/phosphinate structural motif in Medicinal Chemistry. *J. Med. Chem.* **2011**, *54*, 5955–5980. [[CrossRef](#)] [[PubMed](#)]
3. Boughaba, S.; Aouf, Z.; Bechiri, O.; Mathe-Allainmat, M.; Lebreton, J.; Aouf, N.-E. $\text{H}_6\text{P}_2\text{W}_{18}\text{O}_{62}\cdot 14\text{H}_2\text{O}$ as an efficient catalyst for the green synthesis of α -aminophosphonates from α -amino acids. *Phosphorus Sulfur Silicon Relat. Elem.* **2020**, 1–8. [[CrossRef](#)]

4. Chiminazzo, A.; Borsato, G.; Favero, A.; Fabbro, C.; McKenna, C.E.; Dalle Carbonare, L.G.; Valenti, M.T.; Fabris, F.; Scarso, A. Diketopyrrolopyrrole bis-phosphonate conjugate: A new fluorescent probe for in vitro bone imaging. *Chem. Eur. J.* **2019**, *25*, 3617–3626. [[CrossRef](#)] [[PubMed](#)]
5. Rajkoomar, N.; Murugesan, A.; Prabu, S.; Gengan, R.M. Synthesis of methyl piperazinyl-quinolinyl α -aminophosphonates derivatives under microwave irradiation with Pd-SrTiO₃ catalyst and their antibacterial and antioxidant activities. *Phosphorus Sulfur Silicon Relat. Elem.* **2020**, *195*, 1031–1038. [[CrossRef](#)]
6. Nayab, R.S.; Maddila, S.; Krishna, M.P.; Salam, J.T.; Thaslim, B.S.; Chintha, V.; Wudayagiri, R.; Nagam, V.; Tartte, V.; Chinnam, S. In silico molecular docking and in vitro antioxidant activity studies of novel α -aminophosphonates bearing 6-amino-1,3-dimethyl uracil. *J. Recept. Signal Transduct.* **2020**, *40*, 166–172. [[CrossRef](#)] [[PubMed](#)]
7. Awad, M.K.; Abdel-Aal, M.F.; Atlam, F.M.; Hekal, H.A. Molecular docking, molecular modeling, vibrational and biological studies of some new heterocyclic α -aminophosphonates. *Spectrochim. Acta Part A Mol. Biomol. Spectrosc.* **2019**, *206*, 78–88. [[CrossRef](#)]
8. Jabli, D.; Dridi, K.; Efrif, M.L. Activit  Biologique, r activit  et  tude conformationnelle par RMN (¹H, ¹³C, ³¹P) et DFT des hydrazines phosphoryl es vis- -vis des isothiocyanates. *Phosphorus Sulfur Silicon Relat. Elem.* **2017**, *192*, 103–108. [[CrossRef](#)]
9. Chafai, N.; Chafaa, S.; Benbouguerra, K.; Daoud, D.; Hellal, A.; Mehri, M. Synthesis, characterization and the inhibition activity of a new α -aminophosphonic derivative on the corrosion of XC48 carbon steel in 0.5M H₂SO₄: Experimental and theoretical studies. *J. Taiwan Inst. Chem. Eng.* **2017**, *70*, 331–344. [[CrossRef](#)]
10. Benbouguerra, K.; Chafaa, S.; Chafai, N.; Mehri, M.; Moumeni, O.; Hellal, A. Synthesis, spectroscopic characterization and a comparative study of the corrosion inhibitive efficiency of an α -aminophosphonate and schiff base derivatives: Experimental and theoretical investigations. *J. Mol. Struct.* **2018**, *1157*, 165–176. [[CrossRef](#)]
11. Kaur, G.; Shamim, M.; Bhardwaj, V.; Gupta, V.K.; Banerjee, B. Mandelic acid catalyzed one-pot three-component synthesis of α -aminonitriles and α -aminophosphonates under solvent-free conditions at room temperature. *Synth. Commun.* **2020**, *50*, 1545–1560. [[CrossRef](#)]
12. Maestro, A.; Marigorta, E.M.; Palacios, F.; Vicario, J. α -Iminophosphonates: Useful intermediates for enantioselective synthesis of α -aminophosphonates. *Asian J. Org. Chem.* **2020**, *9*, 538–548. [[CrossRef](#)]
13. Tripolszky, A.; T th, E.; Szab , P.T.; Hackler, L.; Kari, B.; Pusk s, L.G.; B lint, E. Synthesis and in vitro cytotoxicity and antibacterial activity of novel 1,2,3-triazol-5-yl-phosphonates. *Molecules* **2020**, *25*, 2643. [[CrossRef](#)] [[PubMed](#)]
14. Elachqar, A.; El Hallaoui, A.; Roumestant, M.L.; Viallefont, P. Synthesis of heterocyclic α -aminophosphonic acids. *Synth. Commun.* **1994**, *24*, 1279–1286. [[CrossRef](#)]
15. Aouine, Y.; Faraj, H.; Alami, A.; El Hallaoui, A.; Elachqar, A.; El Hajji, S.; Kerbal, A.; Labriti, B.; Martinez, J.; Rolland, V. Synthesis of new triheterocyclic compounds, precursors of biheterocyclic amino acids. *J. Mar. Chim. Heterocycl.* **2008**, *7*, 44–49.
16. Tripolszky, A.; N meth, K.; Szab , P.T.; B lint, E. Synthesis of (1,2,3-triazol-4-yl)methyl phosphinates and (1,2,3-triazol-4-yl)methyl phosphates by copper-catalyzed azide-alkyne cycloaddition. *Molecules* **2019**, *24*, 2085. [[CrossRef](#)]
17. Song, W.; Zheng, N.; Li, M.; Ullah, K.; Zheng, Y. Rhodium(I)-catalyzed azide-alkyne cycloaddition (RhAAC) of internal alkynylphosphonates with high regioselectivities under mild conditions. *Adv. Synth. Catal.* **2018**, *360*, 2429–2434. [[CrossRef](#)]
18. Huisgen, R. *Chimie de la Cycloaddition 1,3-Dipolaire*; Wiley: New York, NY, USA, 1984; p. 1.
19. Bentama, A.; El Hadrami, E.M.; El Hallaoui, A.; Elachqar, A.; Lavergne, J.-P.; Roumestant, M.-L.; Viallefont, P.H. Synthesis of new α -heterocyclic α -amino esters. *Amino Acids* **2003**, *24*, 423–426. [[CrossRef](#)]
20. Achamlale, S.; Elachqar, A.; El Hallaoui, A.; El Hajji, S.; Alami, A.; Roumestant, M.L.; Viallefont, Ph. Synthesis of biheterocyclic α -aminophosphonic acid derivatives. *Phosphorus Sulfur Silicon* **1998**, *140*, 103–111. [[CrossRef](#)]
21. Boukallaba, K.; Elachqar, A.; El Hallaoui, A.; Alami, A.; El Hajji, S.; Labriti, B.; Rolland, V. Synthesis of new α -heterocyclic α -aminophosphonates. *Phosphorus Sulfur Silicon Relat. Elem.* **2006**, *181*, 819–823. [[CrossRef](#)]
22. Boukallaba, K.; Elachqar, A.; El Hallaoui, A.; Alami, A.; El Hajji, S.; Labriti, B.; Rolland, V. Synthesis of α -heterocyclic α -aminophosphonates, part II: Morpholine, piperidine, pyrrolidine, tetrahydrofurylmethylamine, *N*-benzyl-*N*-methylamine, and aniline derivatives. *Phosphorus Sulfur Silicon Relat. Elem.* **2007**, *182*, 1045–1052. [[CrossRef](#)]

23. Achamlale, S.; Alami, A.; Aouine, Y. Structure assignment of *N*-protected 2-(1*H*-1,2,3-triazol-1-yl)-glycine derivatives by chemical and spectroscopic methods. *J. Mar. Chim. Heterocycl.* **2019**, *18*, 61–69.
24. Vorobyeva, D.V.; Karimova, N.M.; Vasilyeva, T.P.; Osipov, S.N.; Shchetnikov, G.T.; Odinets, I.L.; Röschenthaler, G.-V. Synthesis of functionalized α -CF₃- α -aminophosphonates via Cu(I)-catalyzed 1,3-dipolar cycloaddition. *J. Fluor. Chem.* **2010**, *131*, 378–383. [[CrossRef](#)]

Publisher’s Note: MDPI stays neutral with regard to jurisdictional claims in published maps and institutional affiliations.



© 2020 by the authors. Licensee MDPI, Basel, Switzerland. This article is an open access article distributed under the terms and conditions of the Creative Commons Attribution (CC BY) license (<http://creativecommons.org/licenses/by/4.0/>).